Title

Poly (ADP-Ribose) polymerase inhibitor MK-4827 together with radiation as a novel therapy for metastatic neuroblastoma.

Journal

Anticancer Research, 33(3)

ISSN

0250-7005

Authors

Mueller, Sabine
Bhargava, Samhita
Molinaro, Annette M
et al.

Publication Date

2013-03-01

Peer reviewed

Published in final edited form as:
Anticancer Res. 2013 March ; 33(3): 755–762.

Poly (ADP-Ribose) Polymerase Inhibitor MK-4827 together with Radiation as a Novel Therapy for Metastatic Neuroblastoma

Sabine Mueller[1,2,3], **Samhita Bhargava**[5], **Annette M. Molinaro**[3,4], **Xiaodong Yang**[6], **Ilan Kolkowitz**[1], **Aleksandra Olow**[6], **Noor Wehmeijer**[7], **Sharon Orbach**[6], **Justin Chen**[1], **Katherine K. Matthay**[2], and **Daphne A. Haas-Kogan**[3,6]

[1]Department of Neurology, University of California, San Francisco, San Francisco, CA, USA
[2]Department of Pediatrics, University of California, San Francisco, San Francisco, CA, USA
[3]Department of Neurosurgery, University of California, San Francisco, San Francisco, CA, USA
[4]Department of Epidemiology and Biostatistics, University of California, San Francisco, San Francisco, CA, USA [5]Department of Pediatrics, Mt. Sinai Medical Center, New York, NY, USA
[6]Department of Radiation Oncology, University of California, San Francisco, San Francisco, CA, USA [7]Department of Radiation Oncology, Academic Medical Center, Amsterdam, The Netherlands

Abstract

Background/Aim—To assess poly (ADP-ribose) polymerase (PARP) inhibitor MK-4827 together with radiation for the treatment of neuroblastoma.

Material and Methods—Clonogenic survival assays were used to assess MK-4827, radiation and combination thereof in four neuroblastoma cell lines. *In vivo* efficacy was tested in a murine xenograft model of metastatic neuroblastoma. *In vivo* targeted inhibition and biological effects included measurement of cleaved caspase-3, gamma-H2AX, and Ki 67 by immunohistochemistry (IHC) and poly-ADP-ribose by Enzyme-Linked Immunosorbent Assay.

Results—Treatment of neuroblastoma cell lines reduced clonogenicity and resulted in additive effects with radiation. *In vivo* treatment with MK-4827 and radiation prolonged survival ($p<0.01$) compared to single modalities. *In vivo* superiority of MK-4827 plus radiation was further documented by significant elevations of cleaved caspase-3 and γ-H2AX in tumors from the combination group compared to single modality cohorts.

Conclusion—Combination of MK-4827 and radiation might provide effective therapy for children with high-risk neuroblastoma.

Neuroblastoma is the most common extracranial tumor of childhood, with approximately 650 new cases diagnosed each year in the United States. Approximately 50% of patients present with high-risk disease, and show *de novo* resistance or relapse after initially responding to treatment. The prognosis for this subset of patients is poor, with survival rates of approximately 20% (1). Hence, there is a compelling need for novel treatment approaches to improve clinical outcomes for patients with metastatic neuroblastoma.

Correspondence to: Sabine Mueller, Department of Neurology, University of California, San Francisco, 675 Nelson Ring, Sandler Neuroscience Center, UCSF, San Francisco, CA 94148, USA. Tel: +1 415 476 3831 Fax: +1 415 502 4372, muellers@neuropeds.ucsf.edu.

Conflict of Interest Notification

Dr. Haas-Kogan has received funding from Merck Oncology to perform laboratory investigations. The study sponsors had no involvement in the study design, collection of the data, analysis or interpretation of the data.

Currently, radiotherapy is used after surgical resection of the primary tumor to prevent local relapse, and for sites of residual metastatic disease after chemotherapy. Radiation causes single- (SSB) and double-strand breaks (DSB) in DNA that are usually repaired by the base excision repair pathway (BER), non-homologous end-joining (NHEJ), or homologous recombination pathway (HR) (2). In response to DNA damage, poly (ADP-ribose) polymerase (PARP)-1, a nuclear enzyme and most abundant member of the PARP family, and PARP-2 rapidly associate with DNA breaks, increasing enzymatic activity by 10- to 500-fold (3). Both histones and PARP are ribosylated in the presence of NAD^+, leading to the formation of negatively charged poly-ADP-ribose (PAR) polymer. PARP facilitates repair of radiation-induced DSBs and therefore PARP inhibitors act as radio sensitizing agents (4, 5). PARP expression is higher in tumor cells than in normal tissues, allowing PARP inhibitors to selectively promote cytotoxic effects in tumor cells, thus increasing the therapeutic index (6). We evaluated the PARP-1 and -2 inhibitor MK-4827 in combination with radiation in a model of metastatic neuroblastoma. We hypothesized that combining MK-4827 with radiation would provide an effective treatment approach for high-risk neuroblastoma. We performed *in vitro* and *in vivo* studies to test this hypothesis.

Materials and Methods

Clonogenic survival assays

Cell lines SH-SY-5Y, Kelly, $NB1691^{luc}$ and Tet 21 were genotyped prior to their use. SH-SY-%Y, Kelly and Tet 21 were a generous gift from Dr. Weiss, San Francisco, CA. $NB1691^{luc}$ were a generous gift from Dr. Davidoff, Memphis, TN. Clonogenic survival assays were carried out as described previously and clinical grade MK-4827 (Merck, Whitehouse Station, NJ, USA) was used for all experiments (7). Doses of irradiation between 0 and 8 Gy were given three hours after MK-4827 administration. MK-4827 was administered at 13 to 38 nM, depending on the IC_{50} of each specific cell line; controls were given an equal amount of DMSO. Surviving fractions were normalized to the plating efficiency of each cell line as previously described (8). The data presented are the mean ± standard deviation (SD) and cells were plated in quadruplicates.

Western blot analysis

Western blot analysis was carried out as described previously (7). Anti-PAR polyclonal antibody (BD Pharmingen, San Diego, CA, USA) was used as primary antibody and goat anti-rabbit IgG horseradish peroxidase (HRP)-conjugated antibody as secondary antibody. The blot was re-probed for β-actin (1:1000) as a loading control.

Immunofluorescence assay for DNA repair marker γ-H2AX

$NB1691^{luc}$ cells were treated at 3, 6, and 24 hours prior to fixation with 2 Gy of radiation and/or 600 nM clinical grade MK-4827. For the radiation plus MK-4827 combination arm, cells were first treated with MK-4827, followed three hours later by radiation, and then harvested, fixed and permeabilized at the indicated time points after irradiation. Cells were incubated with anti-phospho-histone H2AX antibody (Millipore, Billerica, MA, USA) overnight at 4°C followed by incubation with secondary antibody Alexa-Fluor 488-labeled goat anti-mouse IgG antibody (Invitrogen, Grand Island, NY, USA). Nuclear staining was performed with 1.5 μM propidium iodide solution (Invitrogen). Analyses were performed by an INcell 1000 analyzer (GE Healthcare, Madison, WI, USA) examining five random regions per well at x10 magnification. Assays were carried out at each time point in triplicate. Student's *t*-test was used to assess statistically significant differences between treatment groups.

Metastatic neuroblastoma *in vivo* model and treatment

All procedures were performed according to protocols approved by the Institutional Animal Care and Use Committee of the University of California, San Francisco (UCSF). We used an established model of $NB1691^{luc}$ metastatic neuroblastoma in which disease in lymph nodes and liver develop in 100% of mice (7, 9). Forty 5–6 week old female athymic nude Mice (Simonsen Laboratories, Gilroy, CA) were randomized into one of four groups: Ora-Plus (Paddock Laboratories, Minneapolis, MN, USA) carrier control; MK-4827 alone (50 mg/kg by oral gavage for a total of 10 days, Monday-Friday); radiation alone (0.5 Gy 5 daily fractions administered Monday-Friday for a total dose of 2.5 Gy); or MK-4827 plus radiation on the same schedule as the single modality treatment arms. In the combination group, 0.5 Gy of radiation followed one hour after MK-4827 administration for a total of 2.5 Gy. Treatment started seven days after tail vein injection of 6×10^6 $NB1691^{luc}$ cells. Each treatment group contained 10 mice. Tumor volume was monitored as outlined previously (7). The Kaplan–Meier estimator was used to generate survival curves, with differences between survival curves calculated using a log-rank test.

PARP pharmacodynamic assay

The HT PARP *in vivo* pharmacodynamic assay II (Trevigen, Gaithersburg, MD, USA) was performed to quantify PAR in the tumor xenograft samples following the manufacturer's guidelines. Mice with metastatic neuroblastoma were treated with 50 mg/kg of MK-4827 and/or 0.5 Gy of radiation one hour after drug treatment, or with control agent Ora-Plus. Tumors were harvested 24 hours after radiation treatment, and flash frozen in liquid nitrogen to stabilize PAR levels. The assay was carried out in triplicates.

Immunohistochemistry of tumor samples

Tumor samples (multiple liver metastases per mouse) were analyzed from mice treated with 50 mg/kg of MK-4827, 0.5 Gy radiation, 50 mg/kg MK-4827 followed by 0.5 Gy one hour after MK-4827 was given, or Ora-Plus as control. Liver metastases were harvested 24 hours after final treatment, fixed in 4% formalin overnight and processed through ethanolic dehydration series for paraffin embedding. Five micrometer paraffin sections were stained using the following antibodies: anti-gamma-H2AX (Cell Signaling, Boston, MA, USA); anti-cleaved caspase-3 (Cell Signaling), and anti-Ki-67 (Dako, Carpinteria, CA, USA); detected with 3,3′-diaminobenzidine tetrahydrochloride (DAB) substrate (Vector Labs, Burlingame, CA, USA), and counterstained with hematoxylin. Image-based quantification was performed and normalized to that of the control group. Data represent measurements from all metastases present in the section (four in the control group, two in the radiation group, three in the MK-4827 group, and five in the combination treatment group). Up to ten images of areas with the highest numbers of positive cells were taken per tumor (x20; Leica, DMLS microscope, Buffalo Grove, IL, USA) and both positively and negatively stained cells were quantified. Percentages of positive cells were averaged per tumor, and a grand mean of all tumors was normalized to the control (set at 100%). To assess the significance of differences between treatment groups, we first used the Kruskal-Wallis test followed by a Wilcoxon rank sum test for pairwise comparisons.

Results

MK-4827 enhances radiation-induced cytotoxicity in neuroblastoma cells

We first assessed the antiproliferative effects of MK-4827 alone and determined that MK-4827 caused a dose-dependent decrease in clonogenicity of SH-SY-5Y, Kelly, $NB1691^{luc}$ and Tet 21 (without and without doxycycline) cells. The half maximal inhibitory concentration(IC_{50}) ranged from 13 to 38 nM (data not shown) and the IC_{50} for each cell

line was used for the combination experiments with radiation (Figure 1). Figure 1 demonstrates at least additive cytotoxicity produced by combinations of MK-4827 and radiation, independent of V-myc myelocytomatosis viral related gene, neuroblastoma derived (*MYCN*) amplification status.

It is conceivable that higher PARP expression renders cells more sensitive to PARP inhibitors and that PARP expression levels differ between *MYCN* amplified and *MYCN* non-amplified tumors. We therefore interrogated a published gene expression data set and analyzed expression of PARP-1 and PARP-2 (*Gene Expression Omnibus 3960;* GSE3960). We found a significant difference in the expression of PARP-1 between *MYCN* amplified and non-amplified tumors (two-tailed Student's *t*-test $p<0.002$) but no significant difference was seen for PARP-2 (Figure 2).

MK-4827 reduces PAR expression and PARP activity in neuroblastoma cells

When PARP is activated and associates with SSB, it synthesizes PAR polymers, which in turn act as molecular signals to recruit DNA-repair enzymes to mend damaged DNA. As shown in Figure 3, treatment of NB1691^{luc} and Kelly cells with increasing doses of radiation led to increased poly-ADP ribosylation levels, as expected. Treatment with MK-4827 or a combination of MK-4827 and radiation reduced PAR protein expression in Kelly as well as NB1691^{luc} cells, an effect that was present three hours after treatment and lasted up to 24 hours after treatment. PAR polymers appear as a smear due to the different sizes of PAR polymers.

PARP inhibition with MK-4827 increases γ-H2AX expression in neuroblastoma cells

DNA damage caused by ionizing radiation induces rapid phosphorylation of γ-H2AX. Prolonged higher levels of γ-H2AX suggest that DNA repair mechanisms are impaired. To explore the effects of MK-4827 and radiation on DNA repair, we quantified levels of γ-H2AX in NB1691^{luc}cells. Figure 4 demonstrates that combining MK-4827 with radiation led to increased expression levels of γ-H2AX in NB1691^{luc} compared to cells treated with radiation or MK-4827 alone. The levels of γ-H2AX were significantly elevated 24 hours after treatment in cells treated with MK-4827 plus radiation compared to control cells or cells treated with radiation or MK-4927 alone (Student's *t*-test $p < 0.001$). In these cell lines, we also assessed RAD51, another key player in the HR repair pathway but did not find any differences in RAD51 expression among the different treatment arms (data not shown).

Radiosensitization by MK-4827 in an *in vivo* model of metastatic neuroblastoma

To establish the effects of MK-4827 and radiation *in vivo*, we used a model of metastatic neuroblastoma (7). As shown in Figure 5A, combination of MK-4827 and radiation significantly prolonged survival compared to either treatment modalityalone. To document that MK-4827 inhibited PARP activity *in vivo*, we evaluated levels of PAR in tumors removed from NB1691^{luc}-bearing mice following treatment. Both the MK-4827 and the combination group had approximately 200,000 pg/ml PAR, while the radiation group expressed approximately 450,000 pg/ml PAR (Figure 5B). These results indicate that MK-4827 at the dose used in the *in vivo* study, inhibited PARP activity *in vivo* and resulted in the expected biochemical outcome.

Our *in vitro* studies demonstrated that MK-4827 plus radiation increased γ-H2AX levels in neuroblastoma cells (Figure 4). As shown in Figure 6, our *in vivo* results parallel our *in vitro* findings, demonstrating significant increases in γ-H2AX levels in tumors from mice treated with MK-4827 plus radiation compared to those treated with MK-4827 (Wilcoxon rank sum test $p=0.008$) or radiation (Wilcoxon rank sum test $p=0.03$) alone.

To further elucidate the mechanisms of cell death in our *in vivo* model, we performed immunohistochemical staining for cleaved caspase-3 (CC3), a marker of apoptosis. CC3 was significantly increased in tumors from the combination group compared to the MK-4827 (Wilcoxon rank sum p=0.0078) or radiation (Wilcoxon rank sum p=0.0156) treatment arms (see Figure 6C). In addition, Ki 67, a marker of proliferation, was significantly reduced in tumorsfollowing treatment with MK-4827 plus radiation compared to treatment with MK-4827 (Wilcoxon rank sum p=0.0010) or radiation (Wilcoxon Rank Sum p=0.0026) alone.

Discussion

Clinical trials are currently testing PARP inhibitors for the treatment of adult tumors; however, this class of anti cancer agents has been slow to enter the clinic for childhood cancer (10, 11). The favorable toxicity profile of PARP inhibitors and their radiosensitizing effects render them ideal candidates for combination with external beam radiation for a variety of childhood cancer type, or with a targeted radiopharmaceutical, such as ^{131}I - Metaiodobenzylguanidine (^{131}I-MIBG), for neuroblastoma. In this study, we investigated the radiosensitizing effects of the PARP-1/2 inhibitor MK-4827 *in vitro* and in a murine xenograft model of metastatic neuroblastoma. *In vitro*, we demonstrated that combining MK-4827 with radiation increased the efficacy of radiotherapy in a variety of neuroblastoma cell lines independent of their *MYCN* status. While both MK-4827 and radiation had some anti proliferative effects individually, the combination regimen displayed a dose-dependent additive effect. To evaluate any potential correlations between *MYCN* status and response to a PARP1/2 inhibitor, we assessed PARP-1 and PARP-2 expression levels in a published gene expression data set from 20 *MYCN*amplified and 81 *MYCN* non-amplified tumors *(Gene Expression Omnibus 3960)*. We found a significant difference in PARP-1 but not PARP-2 expression between *MYCN* amplified and non-amplified tumors. Additional studies are required to assess whether and how *MYCN* status affects response to PARP inhibition. Prior studies have shown enhanced activity of PARP inhibition in combination with temozolomide and topotecan in neuroblastoma cells but to acknowledge this is the first report of combinations of external beam radiation and PARP inhibition in *in vitro* and *in vivo* models of neuroblastoma (12). Our data are consistent with previous reports of the radio sensitizing effects of PARP inhibitors in other tumor models and support the use of MK-4827 in combination with radiation for the treatment of neuroblastoma (13, 14).

Prior studies have shown that PARP-1 and PARP-2 play roles in a variety of DNA repair pathways such as BER, NHEJ and HR repair (15–18). To assess the effects of MK-4827 on DNA repair in neuroblastoma, we assessed γ-H2AX, a marker of DNA DSBs. Our *in vitro* experiments demonstrated that MK-4827 plus radiation combinations significantlyincreased γ-H2AX expression and our *in vivo* results paralleled these *in vitro* findings and documented augmented γ-H2AX expression after treatment with MK-4827 plus radiation compared to single modality cohorts.

Prior reports have indicated that PARP-1 inhibition down-regulates RAD51, a key factor in the HR repair pathway (18). Contrary to published reports, we did not find a change in RAD51 expression in two independent neuroblastoma cell lines treated with radiation or a combination of radiation plus MK-4827 (data not shown).

In vivo, the combination of MK-4827 and radiation improved survival of mice in a model of metastatic neuroblastoma compared to either single treatment modality. In this *in vivo* model, we were able to assess mechanisms of cooperative anti-neoplastic activity, mode of cell death, and pharmacodynamic effects. The mechanism of combined MK-4827 and radiation activity included augmented inhibition of DNA repair; the mode of cell death

involved apoptotic cell death based on increased CC3 levels, and pharmacodynamic results documented significant down-regulation of PAR in tumors from mice treated with MK-4827 (with or without radiation).

The critical role of radiation in the treatment of high-risk neuroblastoma is well established. In this study, we provide preclinical evidence to support introduction of the PARP-1/2 inhibitor MK-4827 in combination with radiation as therapy for patients with metastatic neuroblastoma. Radiation therapy is one of the mainstays of advanced neuroblastoma treatment, and combining a radio sensitizing agent such as MK-4827 with radiation should increase the efficacy of radiotherapy and potentially improve long-term clinical outcomes.

Acknowledgments

This research was supported in part by the National Institute of Neurological Disorders and Stroke grant K12NS001692 (SM), HHMI (SB), NIH Brain Tumor SPORE grant P50 CA097257 (DHK), Nancy and Stephen Grand Philanthropic Fund (DHK), The V Foundation (KKM, DHK), Merck Inc. (DHK), P01 81403 (KKM), Dougherty Foundation (KKM), Campini Foundation (SM, KKM) and Alex Lemonade Foundation (KKM).

References

1. London WB, Castel V, Monclair T, Ambros PF, Pearson AD, Cohn SL, Berthold F, Nakagawara A, Ladenstein RL, Iehara T, Matthay KK. Clinical and biologic features predictive of survival after relapse of neuroblastoma: a report from the International Neuroblastoma Risk Group project. J Clin Oncol. 2011; 29:3286–3292. [PubMed: 21768459]
2. Kumar R, Horikoshi N, Singh M, Gupta A, Misra HS, Albuquerque K, Hunt CR, Pandita TK. Chromatin modifications and the DNA damage response to ionizing radiation. Front Oncol. 2012; 2:214. [PubMed: 23346550]
3. Krishnakumar R, Kraus WL. The PARP side of the nucleus: molecular actions, physiological outcomes, and clinical targets. Mol Cell. 2010; 39:8–24. [PubMed: 20603072]
4. Calabrese CR, Almassy R, Barton S, Batey MA, Calvert AH, Canan-Koch S, Durkacz BW, Hostomsky Z, Kumpf RA, Kyle S, Li J, Maegley K, Newell DR, Notarianni E, Stratford IJ, Skalitzky D, Thomas HD, Wang LZ, Webber SE, Williams KJ, Curtin NJ. Anticancer chemosensitization and radiosensitization by the novel poly(ADP-ribose) polymerase-1 inhibitor AG14361. J Natl Cancer Inst. 2004; 96:56–67. [PubMed: 14709739]
5. Veuger SJ, Curtin NJ, Richardson CJ, Smith GC, Durkacz BW. Radiosensitization and DNA repair inhibition by the combined use of novel inhibitors of DNA-dependent protein kinase and poly(ADP-ribose) polymerase-1. Cancer Res. 2003; 63:6008–6015. [PubMed: 14522929]
6. Shiobara M, Miyazaki M, Ito H, Togawa A, Nakajima N, Nomura F, Morinaga N, Noda M. Enhanced polyadenosine diphosphate-ribosylation in cirrhotic liver and carcinoma tissues in patients with hepatocellular carcinoma. J Gastroenterol Hepatol. 2001; 16:338–344. [PubMed: 11339428]
7. Mueller S, Yang X, Sottero TL, Gragg A, Prasad G, Polley MY, Weiss WA, Matthay KK, Davidoff AM, DuBois SG, Haas-Kogan DA. Cooperation of the HDAC inhibitor vorinostat and radiation in metastatic neuroblastoma: Efficacy and underlying mechanisms. Cancer Lett. 2011; 306:223–229. [PubMed: 21497989]
8. Franken NA, Rodermond HM, Stap J, Haveman J, van Bree C. Clonogenic assay of cells *in vitro*. Nat Protoc. 2006; 1:2315–2319. [PubMed: 17406473]
9. Dickson PV, Hamner B, Ng CY, Hall MM, Zhou J, Hargrove PW, McCarville MB, Davidoff AM. In vivo bioluminescence imaging for early detection and monitoring of disease progression in a murine model of neuroblastoma. J Pediatr Surg. 2007; 42:1172–1179. [PubMed: 17618876]
10. Dean E, Middleton MR, Pwint T, Swaisland H, Carmichael J, Goodege-Kunwar P, Ranson M. Phase I study to assess the safety and tolerability of olaparib in combination with bevacizumab in patients with advanced solid tumours. Br J Cancer. 2012; 106(3):468–474. [PubMed: 22223088]
11. Samol J, Ranson M, Scott E, Macpherson E, Carmichael J, Thomas A, Cassidy J. Safety and tolerability of the poly(ADP-ribose) polymerase (PARP) inhibitor, olaparib (AZD2281) in

combination with topotecan for the treatment of patients with advanced solid tumors: A phase I study. Invest New Drugs. 2012; 30 (4):1493–1500. [PubMed: 21590367]

12. Daniel RA, Rozanska AL, Thomas HD, Mulligan EA, Drew Y, Castelbuono DJ, Hostomsky Z, Plummer ER, Boddy AV, Tweddle DA, Curtin NJ, Clifford SC. Inhibition of poly(ADP-ribose) polymerase-1 enhances temozolomide and topotecan activity against childhood neuroblastoma. Clin Cancer Res. 2009; 15:1241–1249. [PubMed: 19174487]
13. Efimova EV, Mauceri HJ, Golden DW, Labay E, Bindokas VP, Darga TE, Chakraborty C, Barreto-Andrade JC, Crawley C, Sutton HG, Kron SJ, Weichselbaum RR. Poly(ADP-ribose) polymerase inhibitor induces accelerated senescence in irradiated breast cancer cells and tumors. Cancer Res. 2011; 70:6277–6282. [PubMed: 20610628]
14. Senra JM, Telfer BA, Cherry KE, McCrudden CM, Hirst DG, O'Connor MJ, Wedge SR, Stratford IJ. Inhibition of PARP-1 by Olaparib (AZD2281) increases the radiosensitivity of a lung tumor xenograft. Mol Cancer Ther. 2011; 10:1949–1958. [PubMed: 21825006]
15. Schreiber V, Ame JC, Dolle P, Schultz I, Rinaldi B, Fraulob V, Menissier-de Murcia J, de Murcia G. Poly(ADP-ribose) polymerase-2 (PARP-2) is required for efficient base excision DNA repair in association with PARP-1 and XRCC1. J Biol Chem. 2002; 277:23028–23036. [PubMed: 11948190]
16. Mortusewicz O, Ame JC, Schreiber V, Leonhardt H. Feedback-regulated poly(ADP-ribosyl)ation by PARP-1 is required for rapid response to DNA damage in living cells. Nucleic Acids Res. 2007; 35:7665–7675. [PubMed: 17982172]
17. Mitchell J, Smith GC, Curtin NJ. Poly(ADP-Ribose) polymerase-1 and DNA-dependent protein kinase have equivalent roles in double-strand break repair following ionizing radiation. Int J Radiat Oncol Biol Phys. 2009; 75:1520–1527. [PubMed: 19931734]
18. Hegan DC, Lu Y, Stachelek GC, Crosby ME, Bindra RS, Glazer PM. Inhibition of poly(ADP-ribose) polymerase down-regulates BRCA1 and RAD51 in a pathway mediated by E2F4 and p130. Proc Natl Acad Sci USA. 2010; 107:2201–2206. [PubMed: 20133863]

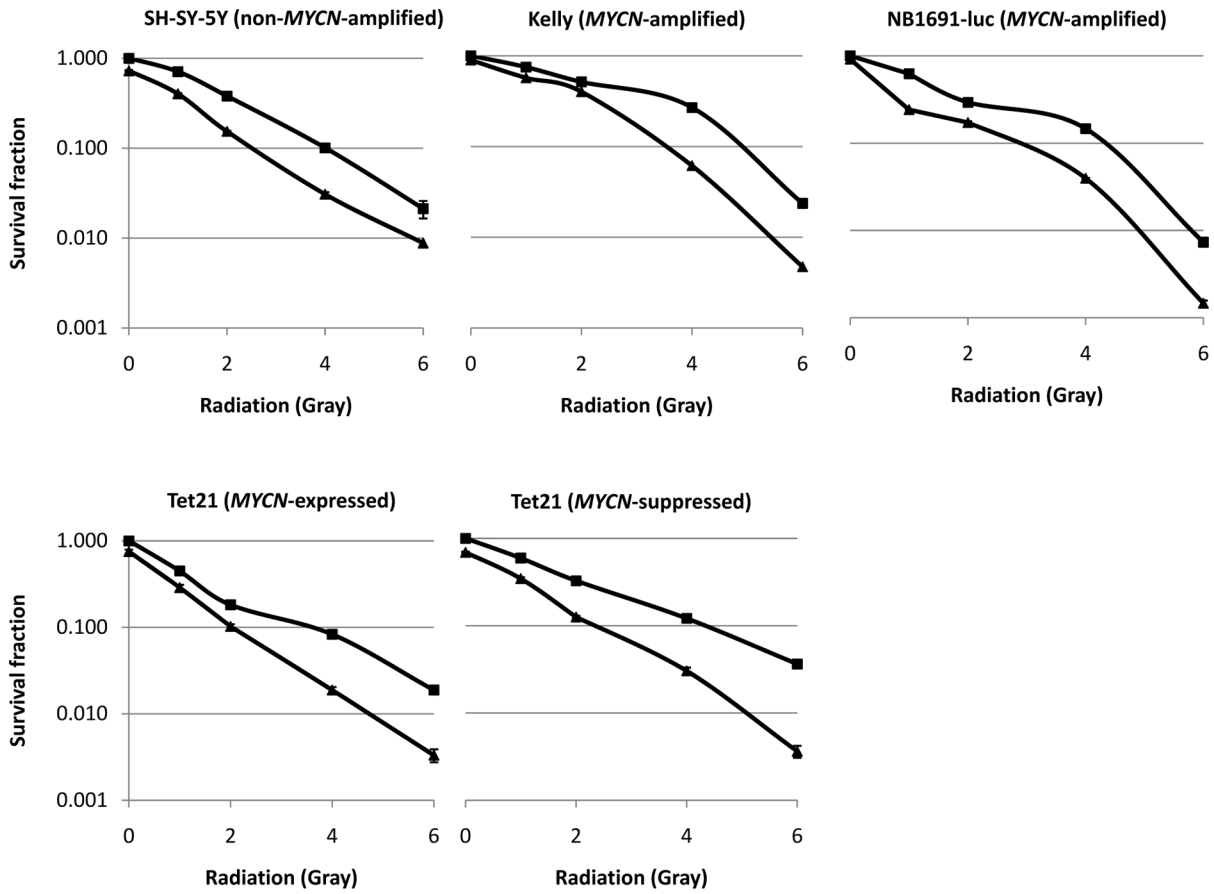

Figure 1. Clonogenic survival assays of neuroblastoma cell lines treated with MK-4827 and radiation

Surviving fractions were normalized to plating efficiency for each cell line and MK-4827 doses were the half maximal inhibitory concentration (IC_{50}) values for each cell line. ■Radiation; ▶MK-4827 plus radiation. All experiments were performed in quadruplicates. Surviving fractions are shown on a log scale as mean values and bars represent the standard error of the mean; where error bars are not visualized, they are smaller than the size of the symbol.

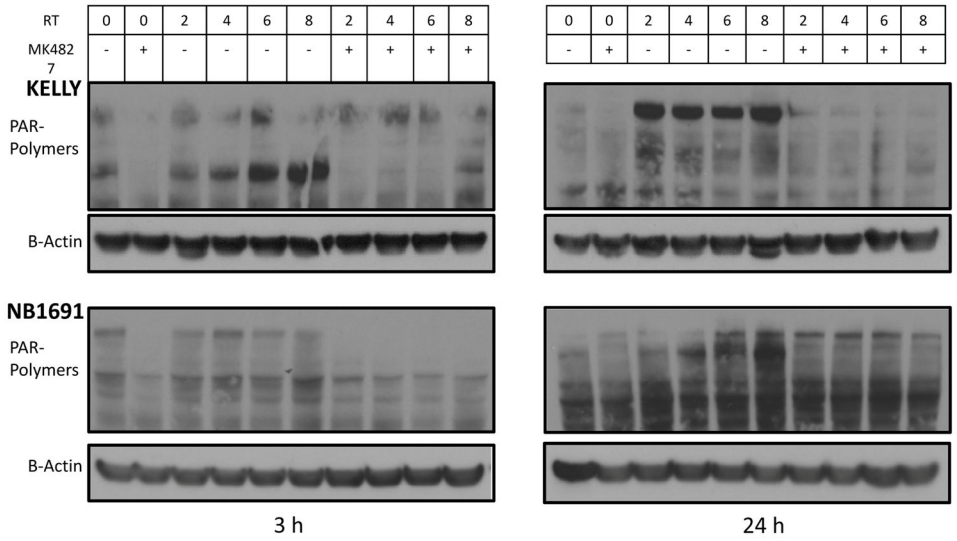

Figure 2. Western blot analysis of poly-ADP-ribose (PAR) in Kelly and NB1691^{luc} cells following treatment with radiation, MK-4827, or combination of MK-4827 plus radiation

NB1691^{luc} and Kelly cells were treated with increasing radiation doses, and 600 nM of MK-4827. In samples undergoing combined treatment, radiation (RT) was given 30 minutes after MK-4827 administration. PAR levels were determined 3 and 24 hours after radiation. β-Actin is shown as loading control.

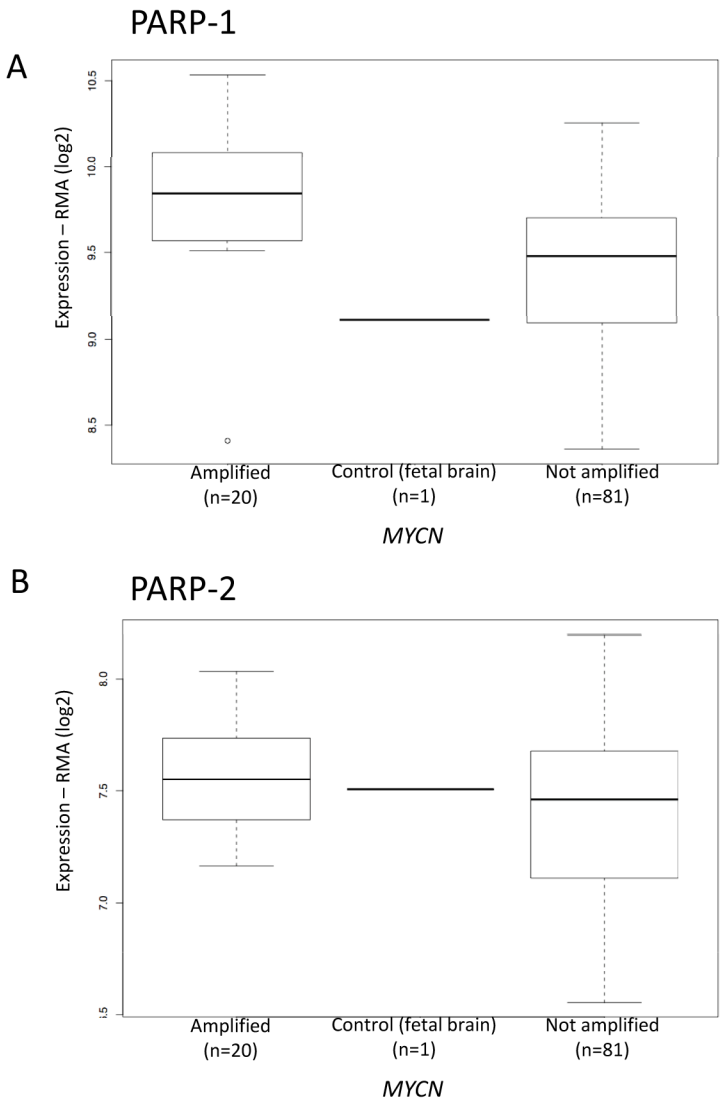

Figure 3. Expression analysis of poly (ADP-ribose) polymerase (PARP)-1 and poly (ADP-ribose) polymerase (PARP)-2 in V-myc myelocytomatosis viral related gene, neuroblastoma derived (*MYCN*) amplified and non-amplified tumors

Expression levels of PARP-1 and PARP-2 were analyzed in a published gene expression data set (*Gene Expression Omnibus 3960;* GSE3960). The analysis started with raw data (CEL files) and applied pre-processing procedure with Robust Multiarray Average. Boxplot graphs for PARP-1 and PARP-2 expression in fetal brain (n=1), *MYCN* amplified (n=20) and *MYCN* non-amplified (n=81) neuroblastoma tumors are shown. Y scale is a log2 transformation of the expression measured and each unit corresponds to a two-fold change in expression. A significant difference in expression levels for PARP-1 expression (two-tailed *t*-test: $p<0.002$) but not for PARP-2 (two-tailed *t*-test: $p=0.159$) was found.

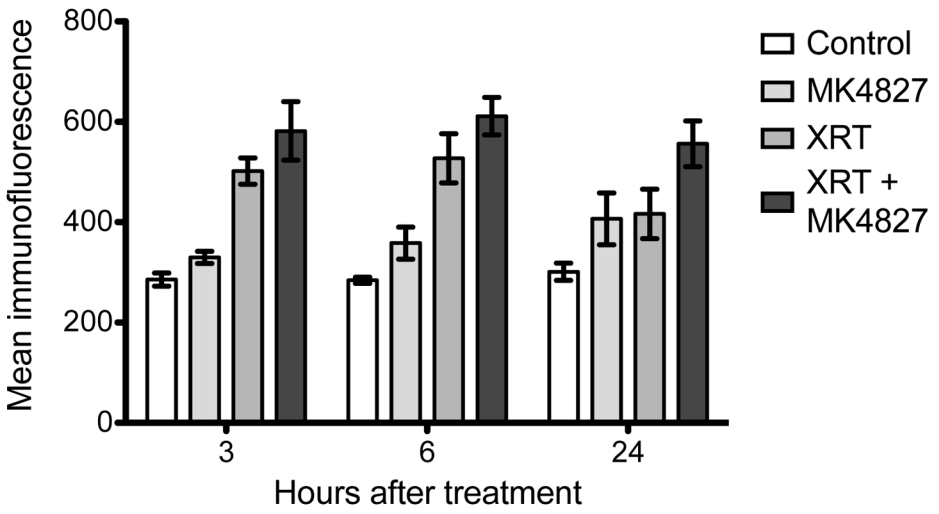

Figure 4. Gamma-H2AX expression after treatment of NB1691^{luc} cells with radiation, MK-4827 or combination of MK-4827 plus radiation

Immunofluorescent quantitation of **γ**-H2AX levels 3, 6, or 24 hours after treatment with MK-4827 (600 nM), radiation (RT; 2 Gy), or MK-4827 followed three hours later by RT. Average immunofluorescence is shown on the y-axis. Data are presented as mean values of triplicate samples and standard deviation. Student's *t*-test was used to assess statistical significance between **γ**-H2AX levels at 24 hours in cells treated with combination of MK-4827 plus radiation compared to radiation ($p<0.001$) or MK-4827 alone ($p<0.001$).

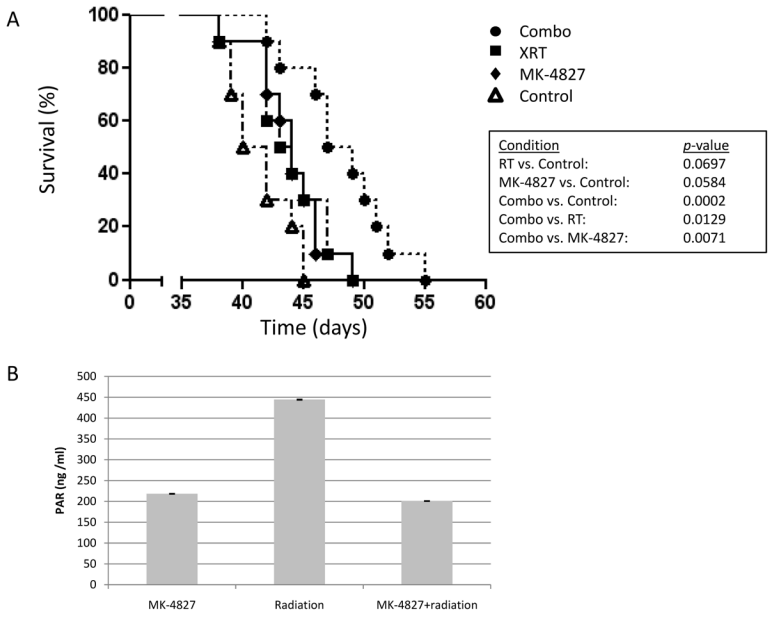

Figure 5. ***In vivo*** **efficacy and target inhibition of combined MK-4827and radiation (RT) in metastatic neuroblastoma**

A: *In vivo* NB1691^{luc} metastases were treated with MK-4827 (50 mg/kg) every day for 10 days; RT (0.5 Gy) every day for 5 days (2.5 Gy total dose); or MK-4827 (50 mg/kg) followed by RT (0.5 Gy delivered one hour after MK-4827); control mice were treated with Ora-Plus only. Kaplan–Meier method was used to generate survival curves, and survival differences between cohorts were calculated using a log-rank test. **B:** *In vivo* poly-ADP-ribose (PAR) levels in tumors 24 hours after treatment with MK-4827 (50 mg/kg), RT (0.5 Gy) or combination therapy [0.5 Gy delivered one hour after MK-4827 (50 mg/kg)]; for each condition tumor samples n=2. The mean and standard deviation for one tumor sample are depicted.

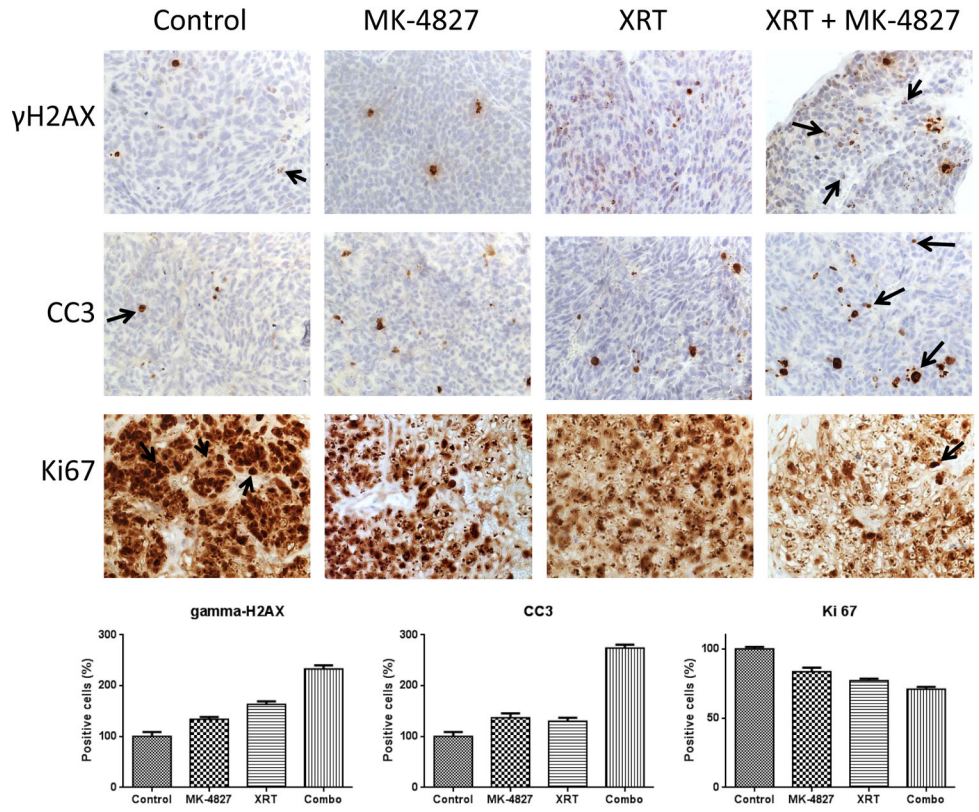

Figure 6. ***In vivo*** **immunohistochemical analyses of gamma H2AX (H2AX), cleaved caspase-3 (CC3) and Ki 67 in human metastatic neuroblastoma xenografts**

A: Representative stains of NB1691^{luc} liver metastases resected 24 hours after MK-4827 (50 mg/kg), RT (0.5 Gy), or MK-4827 (50 mg/kg) followed by RT (0.5 Gy). Arrows indicate positively stained cells. Image-based quantification of γH2AX **(B)**, CC3 **(C),** and Ki67 **(D)** positive tumor cells that were averaged for each tumor and treatment group and normalized to the control (set at 100%). Error bars represent the standard error. Treatment group differences were assessed by Kruskal-Wallis test followed by Wilcoxon rank sum test pairwise comparisons. γH2AX: Combination therapy *versus* control (p<0.0001), RT (p=0.0353), and MK-4827 (p=0.0008). CC3: Combination therapy *versus* control (p=0.0078), RT (p=0.0156); and MK-4827 (p=0.0078). Ki 67: Combination therapy *versus* control (p=0.0156), RT (p=0.0026), and MK-4827 (p=0.0010)